

# Charge-Ordering Phenomena in One-Dimensional Solids

Martin Dressel

1. Physikalisches Institut, Universität Stuttgart,  
Pfaffenwaldring 57, 70550 Stuttgart, Germany

*Email: dressel@pi1.physik.uni-stuttgart.de*

**Abstract.** As the dimensionality is reduced, the world becomes more and more interesting; novel and fascinating phenomena show up which call for understanding. Physics in one dimension is a fascinating topic for theory and experiment: for the former often a simplification, for the latter always a challenge. Various ways will be demonstrated how one-dimensional structures can be achieved in reality. In particular organic conductors could establish themselves as model systems for the investigation of the physics in reduced dimensions; they also have been subject of intensive research at the Dritte Physikalische Institut of Göttingen University over several decades.

In the metallic state of a one-dimensional solid, Fermi-liquid theory breaks down and spin and charge degrees of freedom become separated. But the metallic phase is not stable in one dimension: as the temperature is reduced, the electronic charge and spin tend to arrange themselves in an ordered fashion due to strong correlations. The competition of the different interactions is responsible for which broken-symmetry ground state is eventually realized in a specific compound and which drives the system towards an insulating state.

Here we review the various ordering phenomena and how they can be identified by dielectric and optic measurements. While the final results might look very similar in the case of a charge density wave and a charge-ordered metal, for instance, the physical cause is completely different. When density waves form, a gap opens in the electronic density-of-states at the Fermi energy due to nesting of the one-dimension Fermi-surface sheets. When a one-dimensional metal becomes a charge-ordered Mott insulator, on the other hand, the short-range Coulomb repulsion localizes the charge on the lattice sites and even causes certain charge patterns.

## 1 Introduction

Although the world is three-dimensional in space, physics in one dimension has always attracted a lot of attention. One-dimensional models are simpler compared to three-dimensional ones, and in many cases can be solved analytically only then [1]. Often the reduction of dimension does not really matter because the essential physics remains unaffected. But there are also numerous phenomena in condensed matter which only or mainly occur in one dimension. In general, the dominance

of the lattice is reduced and electronic interactions become superior. Quantum mechanical effects are essential as soon as the confinement approaches the electronic wavelength. Fundamental concepts of physics, like the Fermi liquid theory of interacting particles break down in one dimension and have to be replaced by alternative concepts based on collective excitations [2]. The competition of different interactions concerning the charge, spin, orbital and lattice degrees of freedom can cause ordering phenomena, i.e. phase transitions to a lower-symmetry state as a function of temperature or some order parameter. In one dimension, fluctuations strongly influence the physical properties and smear out phase transitions. An interesting task now is to approximate one-dimensional systems in reality and check the theoretical predictions. Besides pure scientific interest, the crucial importance of these phenomena in nanotechnology might not lie too far ahead.

## 2 Realization of One-Dimensional Systems

### 2.1 Artificial Structures

The ideal one-dimensional system would be an infinite chain of atoms in vacuum; close enough to interact with their neighbors, but completely isolated from the environment. Over the past years, significant progress has been made towards the realization of one-dimensional atomic gases, based on Bose-Einstein condensates of alkalides trapped in two-dimensional optical lattices [3]; however, besides other severe drawbacks, only a limited number of investigations can be performed on quantum gases in order to elucidate their properties.

In solids one-dimensional physics can be achieved in various ways. The most obvious approach would be to utilize semiconductor technology. There layers can be prepared by atomic precision, using molecular beam epitaxy that leads to a two-dimensional electron gas at interfaces and quantum wells [4]. Employing electron-beam lithography and advanced etching technology, one-dimensional quantum wires are fabricated with an effective width comparable to the wavelength of the electrons (Fig. 1). Besides the enormous technological effort, the disadvantage of this approach is that these structures are embedded in bulk materials and not easily accessible to further experiments.

If the surface of a single crystal, like silicon, is cut in a small angle with respect to a crystallographic direction, terraces are produced on the surface with mono-

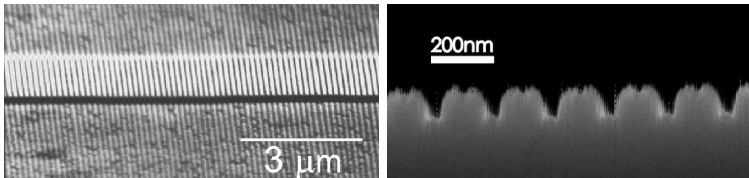


**Figure 1.** One-dimensional semiconductor quantum wells for GaN lasers (electron micrographs provided by H. Schweizer, Stuttgart). (a) The ridge waveguide covers an area of  $1000 \times 6 \mu\text{m}$ ; (b) the second order grating has a period of 190 nm.

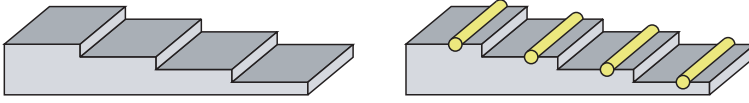


**Figure 2.** Realization of metallic nanowires: The silicon surface is cut in a certain angle leading to single atomic steps; the width of the terrace depends on the angle. Evaporated gold assemble itself in such a way that atomic wires are formed along the steps.

atomic steps separating them. The surface reconstruction may lead to an anisotropic arrangement with the possibility of one-dimensional structures. When a metal, like gold, is evaporated on top of it, the atoms will organize themselves in rows along these steps as visualized in Fig. 2. Taking care of the surface reconstruction and of the right density of gold eventually leads to chains of gold atoms separated by the terrace width [5]. This is a good model of a one-dimensional metal which can be produced in large quantities, easily covering an area of  $1 \times 1 \text{ cm}^2$ . As common in surface technology, ultra-high vacuum is required, and only in situ experiments – like electron diffraction, tunnelling or photoemission spectroscopy – have been performed by now.

One-dimensional topological defects in single crystals, known as dislocations, are an intriguing possibility to achieve a one-dimensional metal, which was utilized by H.-W. Helberg and his group [6] in the frame of the Göttinger Sonderforschungsbereich 126. Dislocations in silicon consist of chains of Si atoms, each having a dangling bond as depicted in Fig. 3, i.e. a non-saturated half-filled orbital [7]. Along these rows, metallic conduction is possible while in the perpendicular direction they are isolated. Since dc measurements with microcontacts on both ends of a single dislocation are challenging, contactless microwave experiments were developed as the prime tool to investigate the electronic transport along dislocations in silicon and germanium [6].

It is possible to grow bulk materials as extremely thin and long hair-like wires when stress is applied; they are known as whiskers of gold, silver, zinc, tin, etc. Metallic whiskers often lead to circuit shortages and failures, and are sought to be avoided. An enormous potential of applications is seen in another sort of filaments solely consisting of carbon atoms: carbon nanotubes. They can be considered as rolled-up sheets of graphite, with electrical properties very much depending on the winding ratio. Single-wall carbon nanotubes with a small diameter and the right winding ratio are excellent realizations of one-dimensional conductors [8].

## 2.2 Anisotropic Crystals

By far the most successful approach to one-dimensional physics are highly anisotropic crystals. Here  $\text{K}_2\text{Pt}(\text{CN})_4\text{Br}_{0.3}\cdot\text{H}_2\text{O}$ , known as KCP, represents the most intuitive example which consists of a chain of platinum ions with overlapping  $d$  orbitals, as depicted in Fig. 4a. The Pt separation is only  $2.894 \text{ \AA}$  along the chain direction while the distance between the chains is  $9.89 \text{ \AA}$ . The Br counterions remove electrons from the planar  $\text{Pt}(\text{CN})_4$  units and the resulting fractional charge  $\text{Pt}^{1.7}(\text{CN})_4$  leads to a partially filled electron band, the prerequisite for metallic behavior. The room

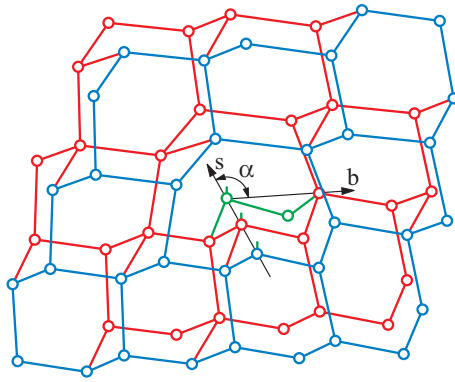


**Figure 3.**  $60^\circ$  dislocation in a (111) plane of a diamond lattice, the Burgers vector points in the direction of **b**. At the edge of the additional plane (indicated by **s**) the covalent bonds have no partner.

temperature conductivity along the chain direction is very high  $\sigma_{\parallel} = 10^2 \text{ } (\Omega\text{cm})^{-1}$ . The anisotropy ratio is  $\sigma_{\parallel}/\sigma_{\perp} = 10^5$  [9].

Transition metal oxides are known for decades to form low-dimensional crystal structures [10]. Varying the composition and structural arrangement provides the possibility to obtain one- and two-dimensional conductors or superconductors, but also spin chains and ladders. The interplay of the different degrees of freedom together with the importance of electronic correlations makes these systems an almost unlimited source for novel and exciting phenomena and a challenge for their theoretical understanding [11]. The blue bronze  $\text{K}_{0.3}\text{MoO}_3$  and related compounds established themselves quickly as model systems to study electronic properties of quasi-one-dimensional metals above and below the Peierls transition at  $T_{\text{CDW}} = 185 \text{ K}$  (Fig. 4b).

While in KCP the metallic properties are due to the platinum ions, organic conductors form a class of solids with no metal atoms present (or relevant); instead the  $\pi$  electrons distributed over of the entire organic molecule form the orbitals which might overlap and lead to band-like conductivity. The additional degree of freedom, tailoring these molecules, supplements the structural arrangement in the crystal and makes it possible to fine-tune competing contributions for the desired properties. This makes organic materials superior for studying low-dimensional physics and ordering phenomena in solids. Low-dimensional organic crystals were explored at the Drittes Physikalisches Institut of Göttingen University already in the 1970s and 1980s; thus in the following we will constrain ourselves mainly to these examples.

In the course of the last two decades, in particular the Bechgaard salts tetra-methyl-tetraselenafulvalene (TMTSF), and its variant TMTTF where selenium is replaced by sulfur, turns out to be an excellent model for quasi-one-dimensional metals, superconductors, charge order, spin-density-wave systems, spin chains, spin-Peierls systems, etc. depending on the degree of coupling along and perpendicular to the chains [12]. The planar organic molecules stack along the  $a$ -direction with a

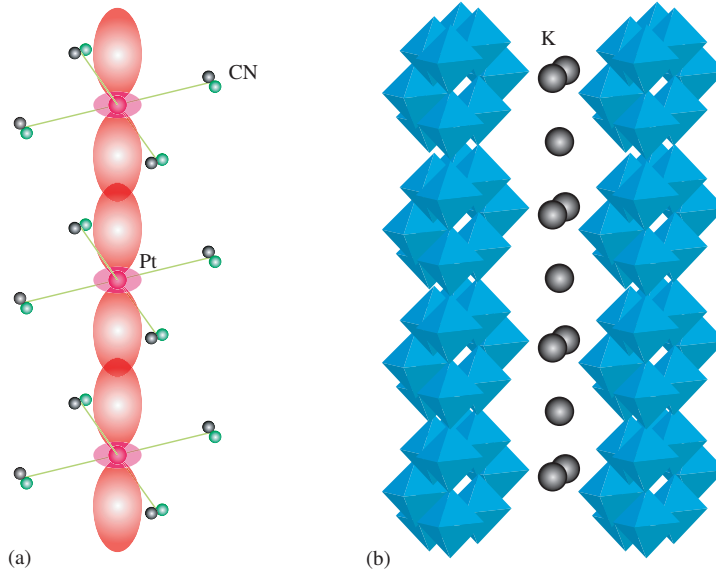


**Figure 4.** (a) In  $\text{K}_2\text{Pt}(\text{CN})_4\text{Br}_{0.3}\cdot\text{H}_2\text{O}$  (KCP) the platinum ions form chains of overlapping orbitals, leading to a metallic conductivity. (b) Sharing edges and corners, the molybdenum oxide octahedra in  $\text{K}_{0.3}\text{MoO}_3$  (blue bronze) form chains along the  $b$  direction. Alkali-ions like K or Rb provide the charge.

distance of approximately  $3.6 \text{ \AA}$ . In the  $b$ -direction the coupling between the chains is small, and in the third direction the stacks are even separated by the inorganic anion, like  $\text{PF}_6^-$ ,  $\text{SbF}_6^-$ ,  $\text{ClO}_4^-$ ,  $\text{Br}^-$ , etc. as depicted in Fig. 5. Each organic molecule transfers half an electron to the counterions. In general, a small dimerization leads to pairs of organic molecules. In addition, spontaneous charge disproportionation, called charge ordering (CO), may divide the molecules into two non-equivalent species (cf. Fig. 11) commonly observed in TMTTF salts. Due to the instability of the quasi one-dimensional Fermi surface, at ambient pressure  $(\text{TMTSF})_2\text{PF}_6$  undergoes a transition to a spin-density-wave (SDW) ground state at  $T_{\text{SDW}} = 12 \text{ K}$ . Applying pressure or replacing the  $\text{PF}_6^-$  anions by  $\text{ClO}_4^-$  leads to a stronger coupling in the second direction: the material becomes more two-dimensional. This seems to be a requirement for superconductivity as first discovered in 1979 by Jérôme and coworkers [12, 13].

### 3 Ordering Phenomena

One-dimensional structures are intrinsically unstable for thermodynamic reasons. Hence various kinds of ordering phenomena can occur which break the translational symmetry of the lattice, charge or spin degree of freedom. On the other hand, fluctuations suppress long-range order at any finite temperature in one (and two) dimension. Only the fact that real systems consist of one-dimensional chains, which

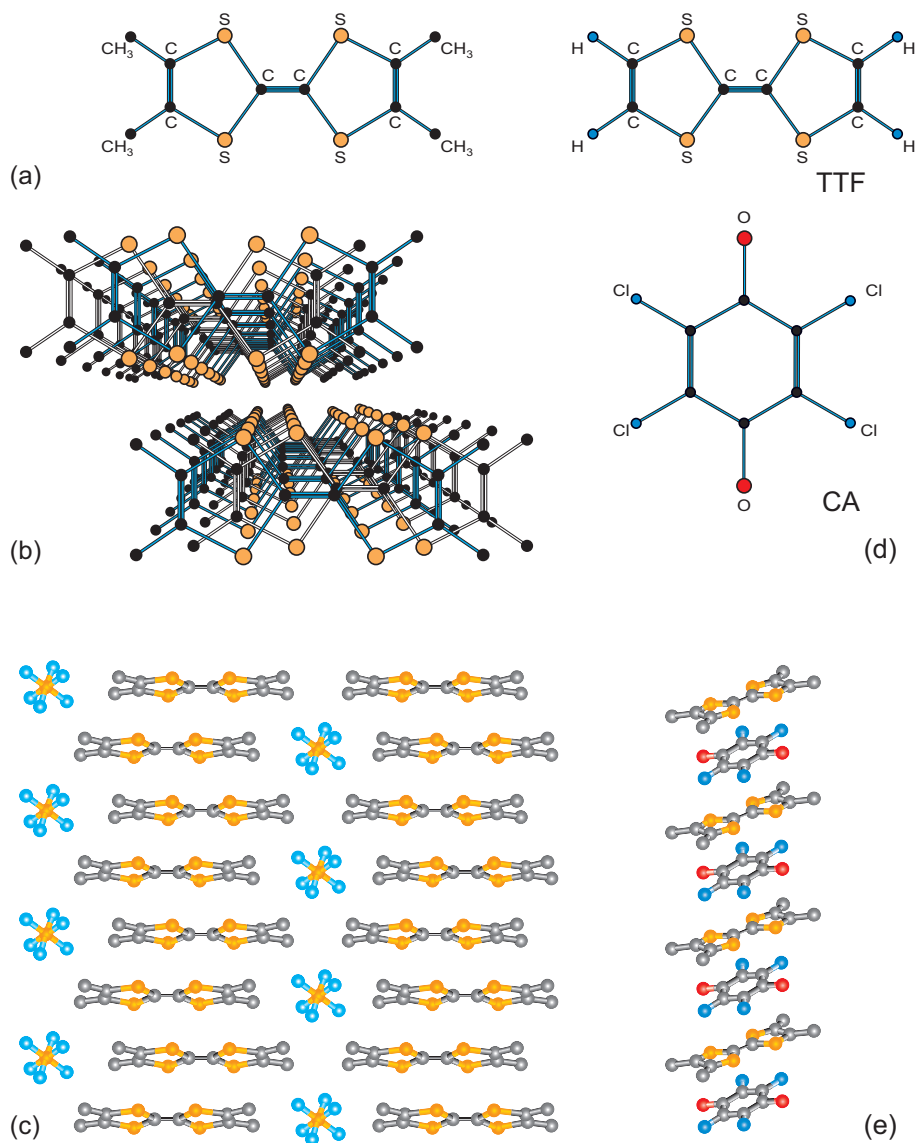


**Figure 5.** (a) Planar TMTTF molecule (b) View along the stacks of TMTTF (*a*-direction) and (c) perpendicular to them (*b*-direction). Along the *c*-direction the stacks of the organic molecules are separated by monovalent anions, like  $\text{PF}_6^-$  or  $\text{AsF}_6^-$ . (d) TTF molecule and chloranil  $\text{QCl}_4$  (e) in the mixed-stack compound TTF-CA, the planar TTF and CA molecules alternate.

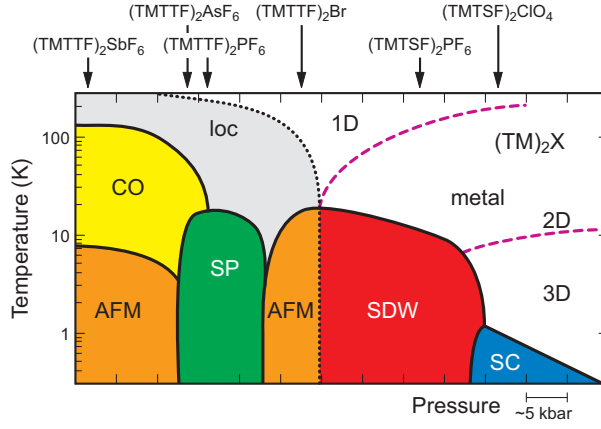


**Figure 6.** The phase diagram of the quasi one-dimensional TMTTF and TMTSF salts. For the different compounds the ambient-pressure position in the phase diagram is indicated. Going from the left to the right by physical or chemical pressure, the materials get less one-dimensional due to the increasing interaction in the second and third direction. Here loc stands for charge localization, CO for charge ordering, SP for spin-Peierls, AFM for antiferromagnet, SDW for spin density wave, and SC for superconductor. The description of the metallic state changes from a one-dimensional Luttinger liquid to a two- and three-dimensional Fermi liquid. While some of the boundaries are clear phase transitions, the ones indicated by dashed lines are better characterized as a crossover.

are coupled to some degree, stabilizes the ordered ground state. The challenge now is to extract the one-dimensional physics from experimental investigations of quasi-one-dimensional systems.

At first glance, there seems to be no good reason that in a chain of molecules the sites are not equivalent, or that the itinerant charges of a one-dimensional metal are not homogeneously distributed. However, the translational symmetry can be broken if electron-phonon interaction and electron-electron interaction become strong enough. Energy considerations then cause a redistribution in one or the other way, leading to charge density waves or charge order. Indeed, these ordering phenomena affect most thermodynamic, transport and elastic properties of the crystal; here we want to focus on the electrodynamic response, i.e. optical properties in a broad sense.

First of all, there will be single-particle electron-hole excitations which require energy of typically an eV. But in addition, collective modes are expected. There is a rather general argument by Goldstone [14] that whenever a continuous symmetry is broken, long-wavelength modulations in the symmetry direction should occur at low frequencies. The fact that the lowest energy state has a broken symmetry means that the system is stiff: modulating the order parameter (in amplitude or phase) will cost energy. In crystals, the broken translational order introduces a rigidity to shear deformations, and low-frequency phonons. These collective excitations are expected well below a meV.

### 3.1 Charge Density Wave

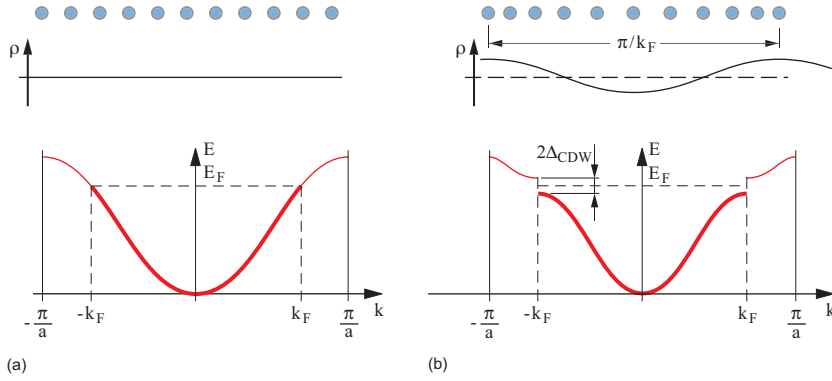


**Figure 7.** (a) In a regular metal, the charge is homogeneously distributed in space. The conduction band is filled up to the Fermi energy  $E_F$ . (b) A modulation of the charge density with a wavelength  $\lambda = \pi/k_F$  changes the periodicity; hence in  $k$ -space the Brillouin zone is reduced which causes a gap  $2\Delta_{CDW}$  at  $\pm k_F$ . The system becomes insulating.

The energy dispersion forms electronic bands which are filled up to the Fermi wave-vector  $\mathbf{k}_F$ . In one dimension, the Fermi surface consists of only two sheets at  $\pm k_F$ . The crucial point is that the entire Fermi surface can be mapped onto itself by a  $2k_F$  translation. Since the density of states in one dimension diverges as  $(E - E_0)^{-1/2}$  at the band-edge  $E_0$ , the electronic system is very susceptible to  $2k_F$  excitations. The result of the Fermi surface nesting and divergency of the electronic density of states is a spatial modulation in the charge density  $\rho(\mathbf{r})$  with a period of  $\lambda = \pi/k_F$  (Fig. 7), which does not have to be commensurate to the lattice: this is called a charge density wave (CDW). Long-range charge modulation is crucial because a CDW is a  $k$ -space phenomenon. Mediated by electron-phonon coupling, this causes a displacement of the underlying lattice (Peierls instability). The gain in electronic energy due to the lowering of the occupied states has to over-compensate the energy required to modulate the lattice [10, 15].

The consequence of the CDW formation is an energy gap  $2\Delta$  in the single-particle excitation spectrum, as observed in the activated behavior of electronic transport or a sharp onset of optical absorption. Additionally, collective excitations are possible which lead to translation of the density wave as a whole. Although pinning to lattice imperfections prevents Fröhlich superconductivity, the density-wave ground state exhibits several spectacular features, like a pronounced non-linearity in the charge transport (sliding CDW) and a strong oscillatory mode in the GHz range of frequency (pinned-mode resonance) [15, 16]. In 1974 this behavior was observed for the first time in the optical properties of KCP [9], but later recovered in all CDW systems. In Fig. 8 the optical reflectivity and conductivity of KCP is displayed for different temperatures and polarizations. Due to the anisotropic nature, the reflectivity  $R(\omega)$  shows a plasma edge only for the electric field  $\mathbf{E}$  along the chains while it remains low and basically frequency independent perpendicular to it, as known



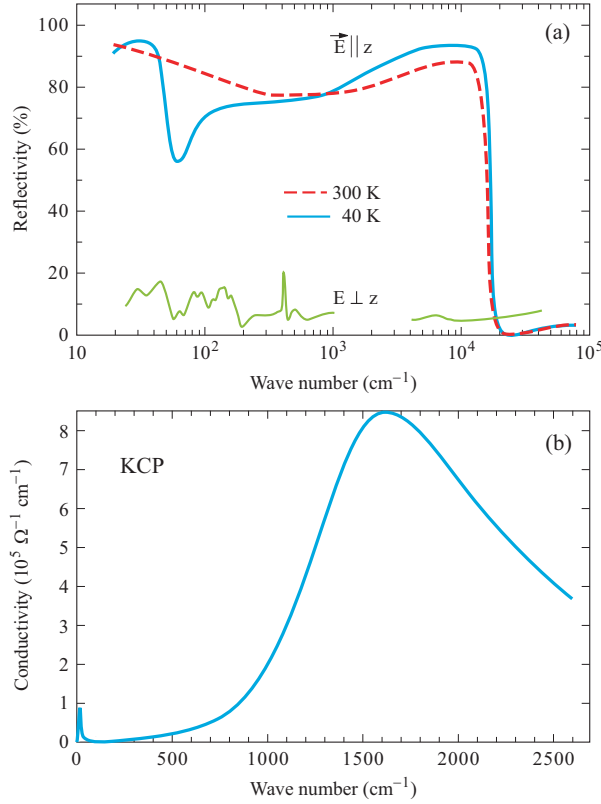


**Figure 8.** (a) Reflectivity of  $\text{K}_2\text{Pt}(\text{CN})_4\text{Br}_{0.3}\cdot\text{H}_2\text{O}$  (abbreviated KCP) measured parallel and perpendicular to the chains at different temperatures as indicated. (b) Optical conductivity of KCP for  $\vec{E} \parallel$  stacks at  $T = 40$  K (after [9]). The excitations across the single-particle Peierls gap lead to a broad band in the mid-infrared while the small and sharp peak centered around  $15 \text{ cm}^{-1}$  is due to the pinned mode.

from dielectrics. At low temperatures, the single particle gap around  $1000 \text{ cm}^{-1}$  becomes more pronounced, and an additional structure is observed in the far-infrared conductivity which is assigned to the pinned-mode resonance induced by the CDW (Fig. 8b).

A detailed investigation of the pinned-mode resonance, its center frequency and lineshape, and furthermore its dependence on temperature and impurity content turned out to be extremely difficult because it commonly occurs in the range of 3 to 300 GHz ( $0.1$  to  $10 \text{ cm}^{-1}$ ); i.e. it falls right into the gap between high-frequency experiments using contacts and optical measurements by freely travelling waves [16]. Microwave technique based on resonant cavities and quasioptical THz spectroscopy was advanced over the years in order to bridge this so-called THz gap [17]. Enclosed resonators have been utilized for decades at the Drittes Physikalisches Institut [18] and were readily available when in 1971 I. Shchegolev suggested them as a tool for

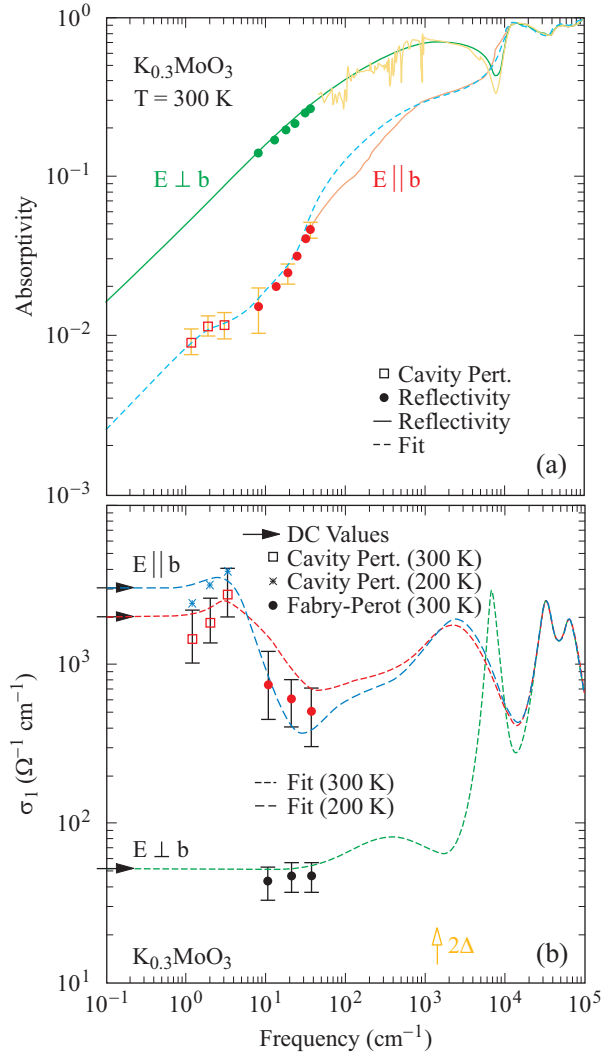


**Figure 9.** (a) Frequency dependence of the room temperature absorptivity  $A = 1 - R$  of blue bronze ( $K_{0.3}MoO_3$ ) in both orientations  $\mathbf{E} \parallel$  stacks and  $\mathbf{E} \perp$  stacks. The squares were obtained by measuring the surface resistance using cavity perturbation method, the circles represent data of quasi-optical reflectivity measurements employing a Fabry-Perot resonator. The solid lines show the results of the dispersion analysis of the data. (b) Optical conductivity of  $K_{0.3}MoO_3$  measured parallel and perpendicular to the stacks by standard dc technique (arrows), cavity perturbation (open squares), coherent-source THz spectroscopy (solid dots) and infrared reflectivity. The open arrow indicates the single-particle gap as estimated from dc measurements below  $T_{CDW}$  (after [20]).

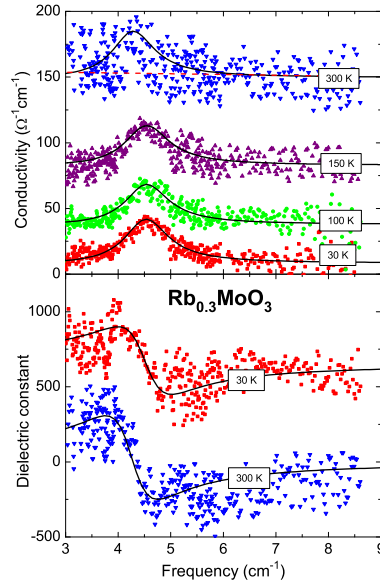


**Figure 10.** Optical conductivity and dielectric constant of  $\text{Rb}_{0.3}\text{MoO}_3$  at various temperatures above and below  $T_{\text{CDW}}$  as indicated; note the curves are *not* shifted. The points represent results directly calculated from the transmission and phase-shift spectra. The solid lines correspond to fits (after [21]). Around  $\omega_0/2\pi c = 4.5 \text{ cm}^{-1}$  the pinned-mode resonance is clearly observed which becomes more pronounced as the temperatures is reduced below  $T_{\text{CDW}} \approx 180 \text{ K}$ . The opening of the single particle gap causes the dielectric constant to increase drastically to approximately 700; the pinned-mode resonance leads to an additional contribution which is present already at room temperature due to fluctuations.

investigating small and fragile low-dimensional organic crystals like TTF-TCNQ [19].

The strong influence of fluctuations in one dimension shifts the actual transition  $T_{\text{CDW}}$  well below the mean-field value  $T_{\text{MF}} = \Delta/1.76k_B$ . This intermediate temperature range  $T_{\text{CDW}} < T < T_{\text{MF}}$  is characterized by the opening of a pseudogap in the density of states, i.e. a reduced intensity close to the Fermi energy which is observed in the magnetic susceptibility but not in dc transport. Optical experiments also see the development of the pseudogap and indications of the collective mode all the way up to  $T_{\text{MF}}$ . Utilizing a combination of different methods, the optical response of  $\text{K}_{0.3}\text{MoO}_3$  was measured parallel and perpendicular to the highly conducting axis; the results for  $T = 300 \text{ K}$  and  $200 \text{ K}$  are displayed in Fig. 9. Clearly pronounced excitations are discovered in the spectra below  $50 \text{ cm}^{-1}$  for the electric field  $\mathbf{E}$  parallel to the chains, the direction along which the charge-density wave develops below the Peierls transition temperature  $T_{\text{CDW}}$ . These excitations are associated with charge-density-wave fluctuations that exist even at room temperature and result in a collective contribution to the conductivity. A single optical experiment finally brought a confirmation of this view: Fig. 10 exhibits results of transmission measurements through thin films of the blue bronze compound  $\text{Rb}_{0.3}\text{MoO}_3$  on an  $\text{Al}_2\text{O}_3$

substrate. The transmission coefficient and phase shift were recorded simultaneously using a Mach-Zehnder interferometer, which is driven by backward wave oscillators as powerful and tunable sources and which operates in the THz range of frequencies (30 GHz to 1500 THz, 1 - 50 cm<sup>-1</sup>) [22].

### 3.2 Charge Order

The crucial point of a CDW is the Fermi surface nesting; the driving force is the energy reduction of the occupied states right below the Fermi energy  $E_F$  when the superstructure is formed (cf. Fig. 7). Well distinct from a charge density wave is the occurrence of charge order (CO). The Coulomb repulsion  $V$  between adjacent lattice sites may lead to the preference of alternatingly more or less charge as depicted in Fig. 11. The extended Hubbard model is a good description of the relevant energies:

$$\mathcal{H} = -t \sum_{j=1} \sum_{\sigma=\uparrow\downarrow} (c_{j,\sigma}^+ c_{j+1,\sigma} + c_{j+1,\sigma}^+ c_{j,\sigma}) + U \sum_{j=1} n_{j\uparrow} n_{j\downarrow} + V \sum_{j=1} n_j n_{j+1} \quad . \quad (1)$$

Here  $t$  denotes the hopping integral to describe the kinetic energy,  $U$  is the on-site Coulomb repulsion, and  $V$  is the nearest neighbor interaction. The disproportionation of charge on the molecules represents a short-range order and has to be commensurate with the lattice. CO may be accompanied by a slight lattice distortion

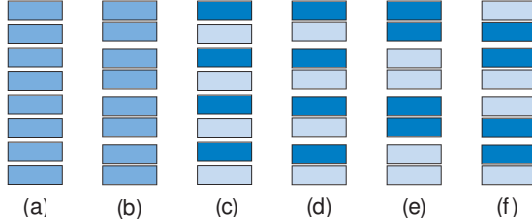


**Figure 11.** Possible arrangement of the molecules along the stacks. The disproportionation of charge is depicted by the different gray shade. The molecules can be dimerized (b), too, which may or may not be accompanied by charge order (c,d). The periodicity doubles again (teramerization) if neighboring dimers carry different charge (e), but also if charge-rich molecules in adjacent dimers form pairs (f).

(Fig. 11d), but this is a secondary effect. In contrast to a CDW, a metallic state above the ordering temperature is not required. If it is the case (metallic state), the gap in the density of states due to the superstructure also causes a metal-insulator transition. The most intriguing example of a charge-order driven metal-to-insulator transition was found in the two-dimensional organic conductor  $\alpha$ -(BEDT-TTF)<sub>2</sub>I<sub>3</sub>, and this kept the community puzzled for almost twenty years. Below  $T_{CO} = 135$  K, the dc and microwave conductivity (first measured in the group of H.-W. Helberg) drops many orders of magnitude (Fig. 12), but no modification in the lattice is observed [23]. Only recently it was understood that electronic correlations are responsible for this phase transition. Optical experiments (Raman and infrared) reveal a charge disproportionation from half a hole per molecule above the phase transition to 0.1e and 0.9e below  $T_{CO}$ ; for a review see Dressel and Drichko [24].

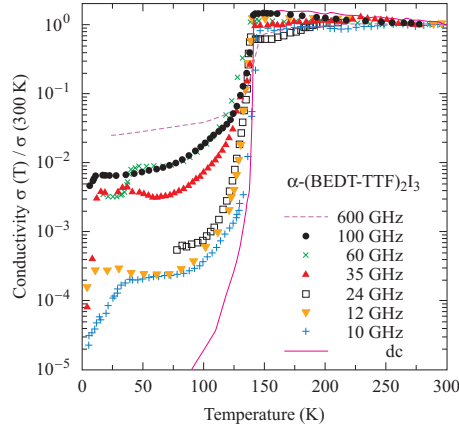


**Figure 12.** Temperature dependent conductivity of  $\alpha$ -(BEDT-TTF) $_2$ I $_3$  within the highly conducting plane measured by dc and microwave technique. The charge-order transition at 135 K leads to a rapid drop of the conductivity. The plateau in the conductivity between 40 K and 100 K increases with frequency indicating hopping conduction (after [23]).

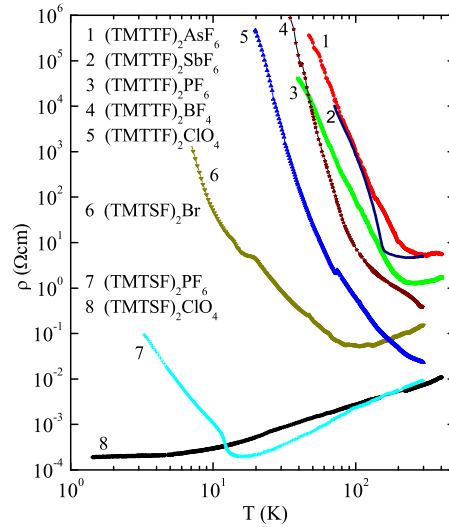


**Figure 13.** Temperature dependence of the dc resistivity of several Fabre and Bechgaard salts. As the temperature is reduced, the charges become increasingly localized in (TMTSF) $_2$ AsF $_6$  and (TMTSF) $_2$ PF $_6$ , before the charge-ordered state is entered below 100 K. (TMTSF) $_2$ SbF $_6$  shows a transition from a metal-like state directly into the charge-ordered state at  $T_{CO} = 150$  K. (TMTSF) $_2$ PF $_6$  undergoes a SDW transition at  $T_{SDW} = 12$  K. Only (TMTSF) $_2$ ClO $_4$  remains metallic all the way down to approximately 1.2 K where it becomes superconducting (after [25]).

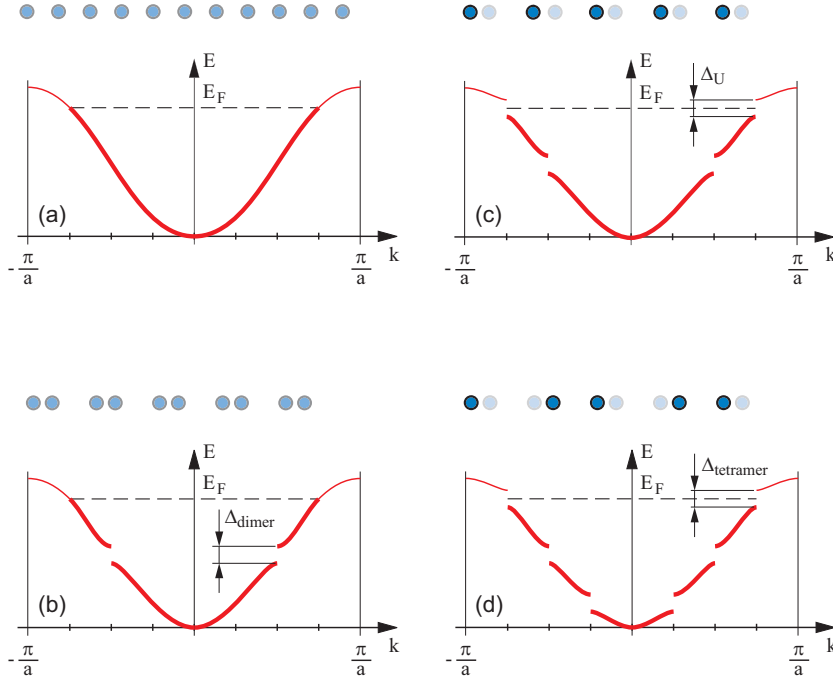


**Figure 14.** (a) A homogeneous stack of TMTCF, for example, with half an electronic charge  $+e$  per molecule results in a three-quarter-filled band which leads to metallic behavior. (b) Dimerization doubles the unit cell and the Brillouin zone is cut into two equal parts. The upper band is half filled and the physical properties remain basically unchanged. (c) Due to on-site Coulomb repulsion  $U$  a gap  $\Delta_U$  opens at the Fermi energy  $E_F$  that drives a metal-to-insulator transition. (d) The tetramerization doubles the unit cell again and also causes a gap  $\Delta_{\text{tetramer}}$ .

Similar phenomena can also be observed in the quasi-one-dimensional  $(\text{TMTTF})_2X$  salts which are poor conductors at ambient temperature and exhibit a rapidly increasing resistivity as the temperature is lowered (Fig. 13). The reason is the accumulation of two effects which severely influence the energy bands as depicted in Fig. 14. The first one is a structural: due to the interaction with the anions (Fig. 5c) the molecular stack is dimerized as visualized in Fig. 11b. The conduction band is split by a dimerization gap  $\Delta_{\text{dimer}}$  and the material has a half-filled band. In a second step the Coulomb repulsion  $V$  causes charge disproportionation within the dimers (Fig. 11d). On-site Coulomb repulsion  $U$  also drives the one-dimensional half-filled system towards an insulating state: correlations induce a gap  $\Delta_U$  at the Fermi energy  $E_F$  as shown in Fig. 14c. The tetramerization of the CO according to Fig. 11e and f changes this picture conceptually (Fig. 14d): the soft gap  $\Delta_{\text{CO}}$  due to short-range nearest-neighbor interaction  $V$  localizes the charge carriers. If not completely developed it just results in a reduction of the density of state (pseudogap). The tetramerization gap, on the other hand, is related to long-range order.

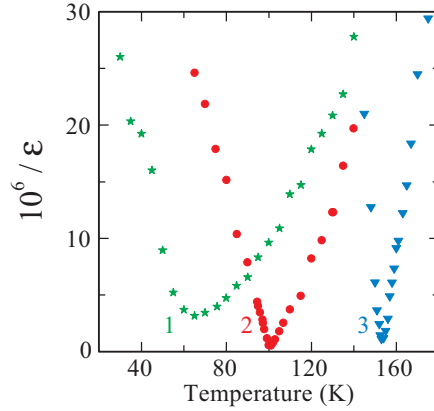


**Figure 15.** Temperature dependence of the inverse dielectric constant  $1/\epsilon$  of  $(\text{TMTTF})_2X$ , with different anions  $X = \text{PF}_6$  (1),  $\text{AsF}_6$  (2), and  $\text{SbF}_6$  (3) (after [27]).

One- and two-dimensional NMR spectroscopy demonstrated the existence of an intermediate charge-ordered phase in the TMTTF family. At ambient temperature, the spectra are characteristic of nuclei in equivalent molecules. Below a continuous charge-ordering transition temperature  $T_{\text{CO}}$ , there is evidence for two inequivalent molecules with unequal electron densities. The absence of an associated magnetic anomaly indicates only the charge degrees of freedom are involved and the lack of evidence for a structural anomaly suggests that charge-lattice coupling is too weak to drive the transition [26].

The first indications of CO came from dielectric measurements in the radio-frequency range [27], where a divergency of the dielectric constant was observed at a certain temperature  $T_{\text{CO}}$ , as depicted in Fig. 15. Since this behavior is well known from ferroelectric transitions, the idea is that at elevated temperatures the molecules carry equivalent charge of  $+0.5e$ ; but upon lowering the temperature, the charge alternates by  $\pm\rho$  causing a permanent dipole moment. Hence, new intermolecular vibrations at far-infrared frequencies below  $100 \text{ cm}^{-1}$  get infrared active along all three crystal axes in the CO state due to the unequal charge distribution on the TMTTF molecules. Above the CO transition, these modes, which can be assigned to translational vibrations of the TMTTF molecules, are infrared silent but Raman active. By now there are no reports on a collective excitation which should show up as a low-frequency phonon.

The CO can be locally probed by intramolecular vibrations. Totally symmetric  $A_g$  modes are not infrared active; nevertheless, due to electron-molecular vibrational (emv) coupling (i.e. the charge transfer between two neighboring organic TMTTF molecules which vibrate out-of phase), these modes can be observed by infrared spectroscopy for the polarization parallel to the stacks. As demonstrated in Fig. 16, the resonance frequency is a very sensitive measure of the charge per molecule [28]. The charge disproportionation increases as the temperature drops below  $T_{\text{CO}}$  in a mean-field fashion expected from a second-order transition; the ratio amounts to

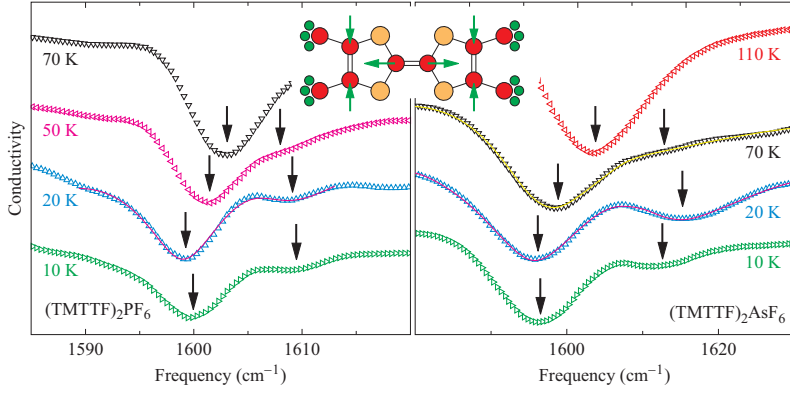


**Figure 16.** Mid-infrared conductivity of  $(\text{TMTTF})_2\text{PF}_6$  and  $(\text{TMTTF})_2\text{AsF}_6$  for light polarized parallel to the molecular stacks. The emv coupled totally symmetric intramolecular  $\nu_3(A_g)$  mode (which mainly involves the C=C double bond) splits due to charge order as the temperature is cooled below  $T_{\text{CO}}$ . The charge disproportionation ratio amounts to about 2:1 in  $(\text{TMTTF})_2\text{AsF}_6$  and 5:4  $(\text{TMTTF})_2\text{PF}_6$  (after [28]).

about 2:1 in  $(\text{TMTTF})_2\text{AsF}_6$  and 5:4  $(\text{TMTTF})_2\text{PF}_6$ . The charge disproportionation is slightly reduced in the  $\text{AsF}_6$  salt, when it enters the spin-Peierls state, and unchanged in the antiferromagnetic  $\text{PF}_6$  salt which infers the coexistence of charge order and spin-Peierls order at low temperatures.

### 3.3 Neutral-Ionic Transition

While in the previous example the crystals consist of separate cation and anion chains between which the electron transfer occurs, mixed-stack organic charge-transfer compounds have only one type of chain composed of alternating  $\pi$  electron donor and acceptor molecules ( $\dots A^{-\rho}D^{+\rho}A^{-\rho}D^{+\rho}A^{-\rho}D^{+\rho}\dots$ ) as sketched in Fig. 5e. These materials are either neutral or ionic, but under the influence of pressure or temperature certain neutral compounds become ionic. There is a competition between the energy required for the formation of a  $D^+A^-$  pair and the Madelung energy. Neutral-ionic (NI) phase transitions are collective, one-dimensional charge-transfer phenomena occurring in mixed-stack charge-transfer crystals, and they are associated to many intriguing phenomena, as the dramatic increase in conductivity and dielectric constant at the transition, such as plotted in Fig. 17 [29, 30].

In the simplest case the charge per molecule changes from completely neutral  $\rho = 0$  to fully ionized  $\rho = 1$ . Ideally this redistribution of charge is decoupled from the lattice, and therefore should not change the inter-molecular spacing. In most real cases, however, the NI transition is characterized by the complex interplay between the average ionicity  $\rho$  on the molecular sites and the stack dimerization  $\delta$ . The ionicity may act as an order parameter only in the case of discontinuous, first order phase transitions. While the inter-site Coulomb interaction  $V$  favors a discontinuous jump of ionicity, the intra-chain charge-transfer integral  $t$  mixes the fully neutral and fully



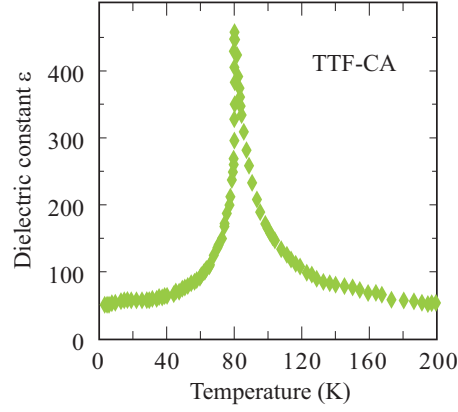


**Figure 17.** Temperature dependent dielectric constant  $\epsilon(T)$  of TTF-CA measured at a frequency of 30 kHz (after [30]). The divergency at  $T_{\text{NI}} = 81$  K clearly evidences the ferroelectric-like neutral-ionic transition.

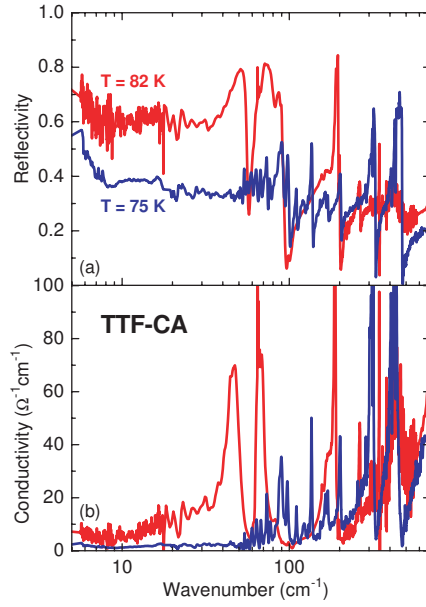


**Figure 18.** (a) Reflectivity and (b) conductivity spectra of TTF-CA measured along the stacking direction above (red line) and below (blue line) the neutral-ionic transition at  $T_{\text{NI}} = 81$  K (after [32]).

ionic quantum states and favors continuous changes in  $\rho$ . The coupling of  $t$  to lattice phonons induces the dimerization of the stack, basically a Peierls-like transition to a ferroelectric state, which is a second order phase transition. Intramolecular (Holstein)

phonons, on the other hand, modulate the on-site energy  $U$  and favor a discontinuous jump in  $\rho$ .

In terms of a modified, one-dimensional Hubbard model [similar to Eq. (1)], the NI transition can be viewed as a transition from a band insulator to a Mott insulator, due to the competition between the energy difference between donor and acceptor sites, and the on-site Coulomb repulsion  $U$ . Peierls and Holstein phonons are both coupled to charge transfer electrons, albeit before the NI transition the former are only infrared active, and the latter only Raman active. This makes polarized Raman and reflection measurements a suitable tool to explore the NI transition.

The temperature induced NI transition of tetrathiafulvalene-chloranil (TTF-CA, cf. Fig. 11d, e) at  $T_{\text{NI}} = 81$  K is the prime example of a first-order transition with a discontinuous jump in  $\rho$ . This can be seen in Fig. 18 by a jump in the frequency of those of the intramolecular vibrations, which are coupled to the electronic charge because their position depends on the charge on the molecules [31, 32].

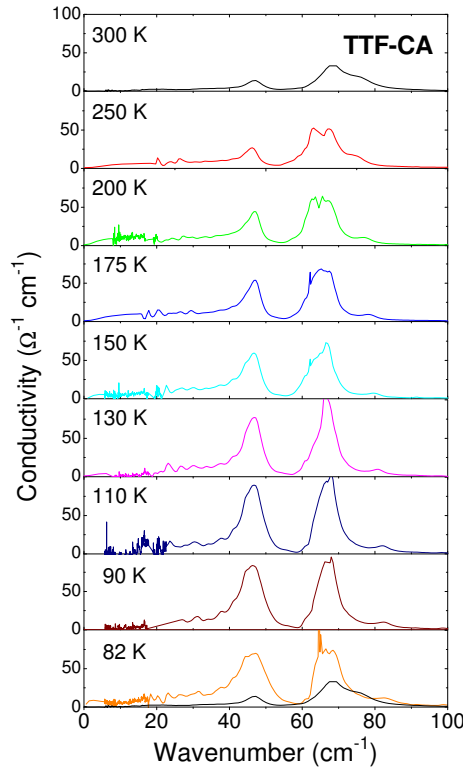


**Figure 19.** Low-frequency conductivity of TTF-CA for  $T > T_{\text{NI}}$  for different temperatures as indicated in the panels. As the NI transition is approached by decreasing temperature, the modes become stronger and an additional band appears as low as  $20 \text{ cm}^{-1}$ . To make the comparison easier, the room temperature spectrum (black line) is replotted in the lowest frame (after [32]).

The vibronic bands present in the infrared spectra for  $T > T_{\text{NI}}$  are combination modes involving the lattice mode, which gives rise to the Peierls distortion at the transition. From calculations we expect three lattice modes which couple to electrons and become stronger as the transition is approached. The lattice modes strongly couple to electrons and behave as soft modes of the ferroelectric transition at  $T_{\text{NI}} = 81$  K. In Fig. 19 the low-frequency conductivity spectra are plotted for different temperatures  $T > T_{\text{NI}}$ . The lowest mode softens most and is seen strongly overdamped around  $20 \text{ cm}^{-1}$ . The temperature evolution of this Peierls mode, which shows a clear softening (from  $70$  to  $20 \text{ cm}^{-1}$ ) before the first-order transition to the ionic ferroelectric state takes place. In the ordered phase, a clear identification and theoretical modelling of the Goldstone mode is still an open problem because the system has several degrees of freedom coupled to each other.

The cooperative charge transfer among the constructive molecules of TTF-CA can also be induced by irradiation of a short laser pulse. A photoinduced local charge-transfer excitation triggers the phase change and cause the transition in both directions [33]. When Cl is replaced by Br in the tetrahalo-*p*-benzoquinones the lattice is expanded, (like a negative pressure) and the ionic phase vanishes completely. Hydrostatic pressure or Br-Cl substitution is utilized as a control parameter to tune the NI transition more or less continuously at  $T \rightarrow 0$  [34].

#### 4 Outlook

No doubt, one-dimensional physics matured from a toy model to an extremely active field of theoretical and experimental research, spanning a broad range from quantum gases to condensed-matter physics and semiconductor technology. Several novel and exciting phenomena can be investigated in these systems. In one-dimensional metals collective modes replace the single-particle excitations common to three-dimensional conductors and described by Landau's Fermi liquid concept of interaction electrons. Another property typical for low-dimensional solids is their susceptibility to symmetry breaking with respect to the lattice, the charge and the spin degrees of freedom. Broken-symmetry ground states imply that the system becomes stiff, because the modulation of the order parameter costs energy; therefore collective modes appear at low energies. In the case of magnets, the broken rotational symmetry leads to a magnetic stiffness and spin waves. In superconductors the gauge symmetry is broken, but due to the Higgs mechanism the Goldstone mode is absent at low frequencies and shifted well above the plasma frequency. In the examples above, we were dealing with translational symmetry, which is lowered in crystals due to charge ordering phenomena.

Charge density waves drive a metal to an insulator, for the Fermi surface becomes instable; the pinned-mode resonance can nicely be detected in the GHz using a variety of high-frequency and optical techniques. Purely electronic correlations between adjacent sites can cause charge disproportionation. Organic conductors are suitable realizations to investigate the properties at the metal-insulator transitions. The neutral-ionic transition observed in mixed-stack one-dimensional organic charge-transfer salts can be a pure change of ionizity, but commonly goes hand in hand with

a Peierls distortion. This can be seen in a softening of the low-frequency phonon modes above the phase transition.

Optical methods and in particular microwave techniques as developed at the Dritte Physikalisches Institut in Göttingen are powerful tools for investigation of charge-ordering phenomena in solids.

**Acknowledgements.** The review is based on many years of collaboration with a large number of people; only some of them can be mentioned here. In particular I would like to thank N. Drichko, M. Dumm, A. Girlando, B. Gorshunov, G. Grüner, and H.-W. Helberg.

## References

- [1] *Mathematical Physics in One Dimension*, edited by E.H. Lieb and D.C. Mattis (Academic Press, New York, 1966).
- [2] T. Giamarchi, *Quantum Physics in One Dimension* (Oxford University Press, Oxford, 2004); M. Dressel, ‘Spin-charge separation in quasi one-dimensional organic conductors’, *Naturwissenschaften* **90**, 337 (2003).
- [3] H. Moritz, T. Stöferle, M. Köhl, and T. Esslinger, ‘Exciting collective oscillations in a trapped 1D gas’, *Phys. Rev. Lett.* **91**, 250402 (2003).
- [4] J.H. Davies, *The Physics of Low-Dimensional Semiconductors* (Cambridge University Press, Cambridge, 1998).
- [5] F.J. Himpsel, A. Kirakosian, J.N. Crain, J.-L. Lin, und D.Y. Petrovykh, ‘Self-assembly of one-dimensional nanostructures at silicon surfaces’, *Solid State Commun.* **117**, 149 (2001).
- [6] M. Dressel and H.-W. Helberg, ‘AC conductivity of deformed germanium single crystals at  $T = 4.2$  K’, *phys. stat. sol. (a)* **96**, K199 (1986); M. Brohl, M. Dressel, H.-W. Helberg, and H. Alexander, ‘Microwave conductivity investigations in plastically deformed silicon’, *Phil. Mag. B* **61**, 97 (1990).
- [7] H. Alexander and H. Teichler, *Dislocations*, in: *Handbook of Semiconductor Technology*, Vol. 1, edited by K.A. Jackson and W. Schröter (Wiley-VCH, New York, 2000), p. 291.
- [8] M. O’Connell, *Carbon Nanotubes* (Taylor & Francis, Boca Raton, 2006); P.J.F. Harris *Carbon Nanotubes and Related Structures* (Cambridge University Press, Cambridge, 2004); S. Reich, C. Thomsen, and J. Maultzsch *Carbon Nanotubes* (Wiley-VCH, Weinheim, 2004).
- [9] P. Brüesch, *Optical Properties of the One-Dimensional Pt Complex Compounds*, in: *One-Dimensional Conductors*, edited by H.G. Schuster (Springer-Verlag, Berlin, 1975), p. 194; P. Brüesch, S. Strässler, and H. R. Zeller, ‘Fluctuations and order in a one-dimensional system. A spectroscopical study of the Peierls transition in  $\text{K}_2\text{Pt}(\text{CN})_4\text{Br}_{0.3}\cdot 3(\text{H}_2\text{O})$ ’, *Phys. Rev. B* **12**, 219 (1975).
- [10] *Electronic Properties of Inorganic Quasi-One-Dimensional Compounds*, Part I/II, edited by P. Monceau, (Reidel, Dordrecht, 1985); *Physics and Chemistry of Low Dimensional Inorganic Conductors*, edited by C. Schlenker, J. Dumas, M. Greenblatt, and S. Van Smalen (Plenum, New York, 1996).
- [11] P.A. Cox, *Transition Metal Oxides* (Clarendon Press, Oxford, 1992); S. Maekawa, T. Tohyama, S.E. Barnes, S. Ishihara, W. Koshibae, and G. Khaliullin, *The Physics of Transition Metal Oxides* (Springer, Berlin, 2004).
- [12] D. Jérôme and H. J. Schulz, ‘Organic conductors and superconductors’, *Adv. Phys.* **31**, 299 (1982); D. Jérôme, in *Organic Conductors*, edited by J.-P. Farges (Marcel Dekker, New York, 1994), p. 405; M. Dressel, ‘Spin-charge separation in quasi one-dimensional

- organic conductors', *Naturwissenschaften* **90**, 337 (2003); M. Dressel, 'Ordering phenomena in quasi one-dimensional organic conductors', *Naturwissenschaften* **94**, DOI 10.1007/s00114-007-0227-1 (2007).
- [13] D. Jérôme, A. Mazaud, M. Ribault, and K. Bechgaard, 'Superconductivity in a synthetic organic conductor (TMTSF)<sub>2</sub>PF<sub>6</sub>', *J. Physique Lett.* **41**, L95 (1980).
  - [14] J. Goldstone, 'Field theories with "superconductor" solution', *Nuovo cimento* **19**, 154 (1961); J. Goldstone, A. Salam, and S. Weinberg, 'Broken symmetries', *Phys. Rev.* **127**, 965 (1962).
  - [15] G. Grüner, *Density Waves in Solids*, (Addison-Wesley, Reading, MA, 1994).
  - [16] M. Dressel and G. Grüner, *Electrodynamics of Solids* (Cambridge University Press, Cambridge, 2002).
  - [17] O. Klein, S. Donovan, M. Dressel, and G. Grüner, 'Microwave cavity perturbation technique. Part I: Principles', *Int. J. Infrared and Millimeter Waves* **14**, 2423 (1993); S. Donovan, O. Klein, M. Dressel, K. Holczer, and G. Grüner, 'Microwave cavity perturbation technique. Part II: Experimental scheme', *Int. J. Infrared and Millimeter Waves* **14**, 2459 (1993); M. Dressel, S. Donovan, O. Klein, and G. Grüner, 'Microwave cavity perturbation technique. Part III: Applications', *Int. J. Infrared and Millimeter Waves* **14**, 2489 (1993); A. Schwartz, M. Dressel, A. Blank, T. Csiba, G. Grüner, A.A Volkov, B.P. Gorshunov, and G.V. Kozlov, 'Resonant techniques for studying the complex electrodynamic response of conducting solids in the millimeter and submillimeter wave spectral range', *Rev. Sci. Instrum.* **66**, 2943 (1995); M. Dressel, O. Klein, S. Donovan, and G. Grüner, 'High frequency resonant techniques for the study of the complex electrodynamic response in solids', *Ferroelectrics* **176**, 285 (1996).
  - [18] H.-W. Helberg and B. Wartenberg, 'Zur Messung der Stoffkonstanten  $\epsilon$  und  $\mu$  im GHz-Bereich mit Resonatoren', *Z. Angew. Phys.* **20**, 505 (1966). The tradition goes back to the Institut für Angewandte Elektrizität (Institute of Applied Electricity) founded in the beginning of the 20th century and headed by Max Reich for a long time. Students like Arthur von Hippel spread this knowledge all around the world and made high-frequency investigations of solids to a powerful tool. The foundation of the *Laboratory of Insulation Research* and the *Radiation Laboratory* at MIT during World War II certainly had the largest impact.
  - [19] L.I. Buranov and I.F. Shchegolev, 'Method of measuring conductivity of small crystals at a frequency of  $10^{10}$  Hz', *Prib. Tekh. Eksp. (engl.)* **14**, 528 (1971); I.F. Shchegolev, 'Electric and magnetic properties of linear conducting chains', *phys. stat. sol (a)* **12**, 9 (1972); H. W. Helberg and M. Dressel, 'Investigations of organic conductors by the Schegolev method', *J. Phys. I. (France)* **6**, 1683 (1996).
  - [20] B.P. Gorshunov, A.A Volkov, G.V. Kozlov, L. Degiorgi, A. Blank, T. Csiba, M. Dressel, Y. Kim, A. Schwartz, and G. Grüner, 'Charge density wave paraconductivity in K<sub>0.3</sub>MoO<sub>3</sub>', *Phys. Rev. Lett.* **73**, 308 (1994); A. Schwartz, M. Dressel, B. Alavi, A. Blank, S. Dubois, G. Grüner, B. P. Gorshunov, A. A. Volkov, G. V. Kozlov, S. Thieme, L. Degiorgi, and F. Lévy, 'Fluctuation effects on the electrodynamics of quasi one-dimensional conductors above the charge-density-wave transition', *Phys. Rev. B* **52**, 5643 (1995).
  - [21] A.V. Pronin, M. Dressel, A. Loidl, H.S.J. van der Zant, O.C. Mantel, and C. Dekker, 'Optical investigations of the collective transport in CDW-films', *Physica B* **244**, 103 (1998).
  - [22] G. Kozlov and A. Volkov, *Coherent Source Submillimeter Wave Spectroscopy*, in: *Millimeter and Submillimeter Wave Spectroscopy of Solids*, edited by G. Grüner (Springer, Berlin, 1998), p. 51; B. Gorshunov, A. Volkov, I. Spektor, A. Prokhorov, A. Mukhin, M. Dressel, S. Uchida, and A. Loidl, 'Terahertz BWO-spectroscopy', *Int. J. of Infrared*

- and Millimeter Waves, **26**, 1217 (2005).
- [23] K. Bender, K. Dietz, H. Endres, H.-W. Helberg, I. Hennig, H.J. Keller, H.W. Schäfer, and D. Schweitzer, ‘(BEDT-TTF) $^{2+}$ J $_3^-$  - A two-dimensional organic metal’, Mol. Cryst. Liq. Cryst. **107**, 45 (1984); M. Dressel, G. Grüner, J.P. Pouget, A. Breining, and D. Schweitzer, ‘Field- and frequency dependent transport in the two-dimensional organic conductor  $\alpha$ -(BEDT-TTF) $_2$ I $_3$ ’ J. de Phys. I (France) **4**, 579 (1994).
  - [24] M. Dressel and N. Drichko, ‘Optical properties of two-dimensional organic conductors: signatures of charge ordering and correlation effects’, Chem. Rev. **104**, 5689 (2004); M. Dressel, ‘Ordering phenomena in quasi one-dimensional organic conductors’, Naturwissenschaften **94**, DOI 10.1007/s00114-007-0227-1 (2007).
  - [25] M. Dressel, S. Kirchner, P. Hesse, G. Untereiner, M. Dumm, J. Hemberger, A. Loidl, and L. Montgomery ‘Spin and charge dynamics in Bechgaard salts’, Synth. Met. **120**, 719 (2001).
  - [26] D.S. Chow, F. Zamborszky, B. Alavi, D.J. Tantillo, A. Baur, C.A. Merlic, and S.E. Brown, ‘Charge ordering in the TMTTF family of molecular conductors’, Phys. Rev. Lett. **85**, 1698 (2000).
  - [27] P. Monceau, F. Ya. Nad, and S. Brazovskii, ‘Ferroelectric Mott-Hubbard phase of organic (TMTTF) $_2$ X conductors’, Phys. Rev. Lett. **86**, 4080 (2001).
  - [28] M. Dumm, M. Abaker, and M. Dressel, ‘Mid-infrared response of charge-ordered quasi-1D organic conductors (TMTTF) $_2$ X’, J. Phys. IV (France) **131**, 55 (2005).
  - [29] J.B. Torrance, J.E. Vazquez, J.J. Mayerle, and V.Y. Lee, ‘Discovery of a neutral-to-ionic phase transition in organic materials’, Phys. Rev. Lett. **46**, 253 (1981); J.B. Torrance, A. Girlando, J.J. Mayerle, J.I. Crowley, V.Y. Lee, P. Batail, and S.J. LaPlace, ‘Anomalous nature of neutral-to-ionic phase transition in tetrathiafulvalene-chloranil’, Phys. Rev. Lett. **47**, 1747 (1981); T. Mitani, Y. Kaneko, S. Tanuma, Y. Tokura, T. Koda, and G. Saito, ‘Electric conductivity and phase diagram of a mixed-stack charge-transfer crystal: Tetrathiafulvalene-p-chloranil’, Phys. Rev. B **35**, 427 (1987); S. Horiuchi, Y. Okimoto, R. Kumai, and Y. Tokura, ‘Anomalous valence fluctuation near a ferroelectric transition in an organic charge-transfer complex’, J. Phys. Soc. Japan **69**, 1302 (2000).
  - [30] S. Horiuchi, Y. Okimoto, R. Kumai, and Y. Tokura, ‘Anomalous valence fluctuation near a ferroelectric transition in an organic charge-transfer complex’, J. Phys. Soc. Jpn. **69**, 1302 (2000).
  - [31] M. Masino, A. Girlando, and Z.G. Soos, ‘Evidence for a soft mode in the temperature induced neutral-ionic transition of TTF-CA’, Chem. Phys. Lett. **369**, 428 (2003).
  - [32] M. Masino, A. Girlando, A. Brillante, R.G. Della Valle, E. Venuti, N. Drichko, and M. Dressel, ‘Lattice dynamics of TTF-CA across the neutral ionic transition’, Chem. Phys. **325**, 71 (2006); N. Drichko *et al.*, to be published.
  - [33] S.Y. Koshihara, Y. Takahashi, H. Saki, Y. Tokura, and T. Luty, ‘Photoinduced cooperative charge transfer in low-dimensional organic crystals’, J. Phys. Chem. B **103**, 2592 (1999).
  - [34] S. Horiuchi, Y. Okimoto, R. Kumai, and Y. Tokura, ‘Quantum phase transition in organic charge-transfer complexes’, Science **299**, 229 (2003).